COLD SPRING HARBOR
Molecular Case Studies

RESEARCH REPORT

Genome sequencing identifies three molecular diagnoses including a mosaic variant in the *COL2A1* gene in an individual with Pol III–related leukodystrophy and Feingold syndrome

Kayla J. Muirhead,[1,3] Amanda R. Clause,[2,3] Zinayida Schlachetzki,[2,3] Holly Dubbs,[1] Denise L. Perry,[2] R. Tanner Hagelstrom,[2] Ryan J. Taft,[2] and Adeline Vanderver[1]

[1]Children's Hospital of Philadelphia, Philadelphia, Pennsylvania 19104, USA; [2]Illumina Clinical Services Laboratory, Illumina Inc., San Diego, California 92122, USA

Abstract Undiagnosed genetic disease imposes a significant burden on families and health-care resources, especially in cases with a complex phenotype. Here we present a child with suspected leukodystrophy in the context of additional features, including hearing loss, clinodactyly, rotated thumbs, tapered fingers, and simplified palmar crease. Trio genome sequencing (GS) identified three molecular diagnoses in this individual: compound heterozygous missense variants associated with polymerase III (Pol III)–related leukodystrophy, a 4-Mb de novo copy-number loss including the *MYCN* gene associated with Feingold syndrome, and a mosaic single-nucleotide variant associated with *COL2A1*-related disorders. These variants fully account for the individual's features, but also illustrate the potential for superimposed and unclear contributions of multiple diagnoses to an individual's overall presentation. This report demonstrates the advantage of GS in detection of multiple variant types, including low-level mosaic variants, and emphasizes the need for comprehensive genetic analysis and detailed clinical phenotyping to provide individuals and their families with the maximum benefit for clinical care and genetic counseling.

Corresponding author:
vandervera@chop.edu

Ontology terms: abnormal CNS myelination; aggressive behavior; bilateral single transverse palmar creases; central hypotonia; cerebral hypomyelination; clinodactyly of the 5th finger; failure to thrive in infancy; malar flattening; microcephaly; recurrent otitis media; short chin; tapered finger

Published by Cold Spring Harbor Laboratory Press

doi:10.1101/mcs.a006143

INTRODUCTION

Although Mendelian disorders are individually rare, an estimated 2%–7% of individuals who undergo exome sequencing (ES) receive more than one molecular diagnosis (Yang et al. 2013, 2014; Balci et al. 2017; Ferrer et al. 2019; Posey et al. 2019; Smith et al. 2019). Individuals with multiple molecular diagnoses can present with both distinct and overlapping phenotypes, which challenges providers seeking an etiology, especially in the rare disease community. In some cases, the phenotypic overlap of distinct disease entities in a single individual may be mistaken as previously unreported phenotypic variation for one disease (Yang et al. 2014). The clinician's assessment and understanding of the individual's

[3]These authors contributed equally to this work.

phenotype impact genetic test selection and interpretation (Yang et al. 2014; Posey et al. 2016; Jehee et al. 2017). Choice of the initial genetic test can thus constrain the results and therefore the medical advice provided.

The genetic variation contributing to any given molecular diagnosis is diverse and can include both copy-number variants (CNVs) as well as small variants (single-nucleotide variants [SNVs] and indels) in the nuclear or mitochondrial genomes. Genome sequencing (GS) can detect multiple variant types in a single assay, including SNVs, CNVs, indels, mitochondrial variants, and short tandem repeats (STRs) (Roller et al. 2016; Dolzhenko et al. 2017; Gross et al. 2019). In addition, somatic mosaicism identified through ES and GS has been reported in several studies (Miller et al. 2020; Rodin et al. 2021).

Currently, the American College of Medical Genetics and Genomics (ACMG) recommends that children with one or more congenital anomalies with onset prior to 1 yr of age and/or with developmental delay pursue ES or GS as a first- or second-tier test, with GS offering a more favorable performance in respect to overall diagnostic yield (Manickam et al. 2021). In individuals with white matter disorders, GS has been shown to decrease time to diagnosis, improve diagnostic efficacy, and potentially increase diagnostic yield compared to ES by 6%–9% (Helman et al. 2020; Vanderver et al. 2020).

This report describes an individual who presented with a suspected white matter disorder and additional unexplained phenotypic features that prompted first-line GS testing. Three molecular diagnoses were revealed, including a compound heterozygous (CH) missense variant pair associated with leukodystrophy, a large CNV loss, and a clinically unsuspected mosaic SNV.

RESULTS

Clinical Presentation and Family History

The white European child of interest in this case report was born full term to a gravida one mother by planned cesarean delivery because of breech presentation. The child's prenatal ultrasound was concerning for signs of trisomy 21, but subsequent postnatal high-resolution chromosome analysis (g-banding $\geq$ 650) showed a normal female result (46,XX) with no apparent structural abnormality or rearrangement. The child presented with concern for microcephaly at birth, but this was initially attributed to familial variation, as the mother also presented with a relatively small head size.

Early history was remarkable for delayed dentition and concern for craniosynostosis given the child's small head size. At 10 mo of age, initial tooth eruption was reported. At 13 mo of age, a skull X-ray was performed because of concern for craniosynostosis, which was not substantiated as the sagittal, lambdoid, and coronal sutures were patent and the anterior fontanelle was almost closed.

All gross and fine motor milestones were reportedly on time, but language was delayed. In terms of gross motor skills, the following were reported: ability to sit without support at 5 mo, stand alone at 10 mo, walk independently at 11 mo, and walk upstairs at 18 mo. In respect to fine motor skills, the child was able to put hands together and reach for objects at 3 mo and use a pincer grasp at 8 mo. At 18 mo the child was able to say "mama" and "dada" but lacked additional words. At this time, evaluation by a neurologist was performed in the context of language delay and clinically confirmed microcephaly, but no brain imaging was ordered.

In the interim, the child continued to progress in speech, particularly following bilateral myringotomy with placement of ear tubes recommended because of recurrent otitis media and mild to moderate hearing loss confirmed via audiogram. Behavioral issues, including aggressive behavior and difficulties in communication, were reported. In addition, a diagnosis

of sensory processing disorder was made. Because of her pediatrician's persistent concern for microcephaly, a brain magnetic resonance imaging (MRI) was performed at 2 yr and 6 mo of age. Imaging showed significant hypomyelination with T2 hyperintensity throughout the cortical white matter accompanied by T2 hypointensity affecting the lateral thalamus and medial globus pallidus, consistent with a hypomyelinating leukodystrophy and suggestive of polymerase III (Pol III)–related leukodystrophy (Fig. 1A–C; Steenweg et al. 2010; Vrij-Van Den Bos et al. 2017).

At 2 yr and 7 mo old, the child was evaluated by specialists in the Leukodystrophy Center at the Children's Hospital of Philadelphia in the context of a suspected white matter disorder. Clinical presentation to date was remarkable for microcephaly, oral fixation, impaired body awareness, aggressive behavior, hypotonia, mild dysmorphic features (reduced malar prominence, small chin, abnormal interocular distance, clinodactyly of the fifth finger, tapered fingers, simplified palmar creases, and rotated thumb), delayed dentition, poor weight gain, and mild axial hypotonia. Measurements were weight 11.6 kg (11th centile), height 92 cm (58th centile), and head circumference 43 cm (<3rd centile) per Centers for Disease Control (CDC) U.S. growth charts (Kuczmarski et al. 2002). No family history relevant to the child's clinical presentation was reported (Fig. 1D).

Genomic Analyses

Trio clinical genome sequencing was performed, and four variants were reported (Table 1): a compound heterozygous pair of missense variants in the *POLR3B* gene (NM_018082.6), c.1568T > A (p.Val523Glu), and c.2278G > A (p.Ala760Thr); a de novo heterozygous 4-Mb loss of 2p24.3p24.1; and a de novo missense variant in *COL2A1* (NM_001844.5), c.1693C > T (p.Arg565Cys), which was suspected to be mosaic because of its low variant allele fraction (Table 2; Fig. 1E). The true de novo status of the variant was confirmed by multiple inherited rare variants within the trio as well as quality metrics for the variant.

The *POLR3B* gene encodes RNA Pol III subunit B, the second largest subunit of RNA polymerase III. Together with the subunit encoded by *POLR3A*, POLR3B forms the catalytic core of the polymerase and functions in the transcription of ribosomal RNA (rRNA) and transfer RNA (tRNA). Variation in the *POLR3B* gene is associated with RNA Pol III–related leukodystrophy, a condition with autosomal recessive inheritance characterized by hypomyelination and progressive neurological symptoms (Bernard and Vanderver 2017). Clinical features include progressive motor decline, tremor, ataxia, and cognitive regression. Other common features include hypodontia, ocular and eye movement abnormalities, and hypogonadotropic hypogonadism. Onset is typically in early childhood, but a small minority of affected individuals can have a later onset between 5 yr of age and adolescence or early adulthood. The severity of symptoms can vary among affected individuals of the same family. Variants in the *POLR3B* gene account for ~50% of cases and are typically associated with an earlier onset but slower disease progression. Although cerebellar atrophy is typically observed with *POLR3B* variants, this finding is variable in severity and is not always present (Wolf et al. 2014).

The paternally inherited *POLR3B* p.Val523Glu variant was classified as pathogenic based on its documented association with Pol III–related leukodystrophy in at least 70 affected individuals and application of the ACMG criteria (Table 1; Battini et al. 2012; Daoud et al. 2013; Wolf et al. 2014). This variant has been linked to a common ancestral haplotype and associated with a milder phenotype. It is reported at a maximum frequency of 0.000605 in the European (non-Finnish) population of gnomAD (v2.1.1). The maternally inherited *POLR3B* p.Ala760Thr variant had not been previously reported in the literature and is reported at a maximum frequency of 0.000059 in the European (non-Finnish) population of gnomAD (v3.1.1). This variant was classified as likely pathogenic based on its rarity, identification in

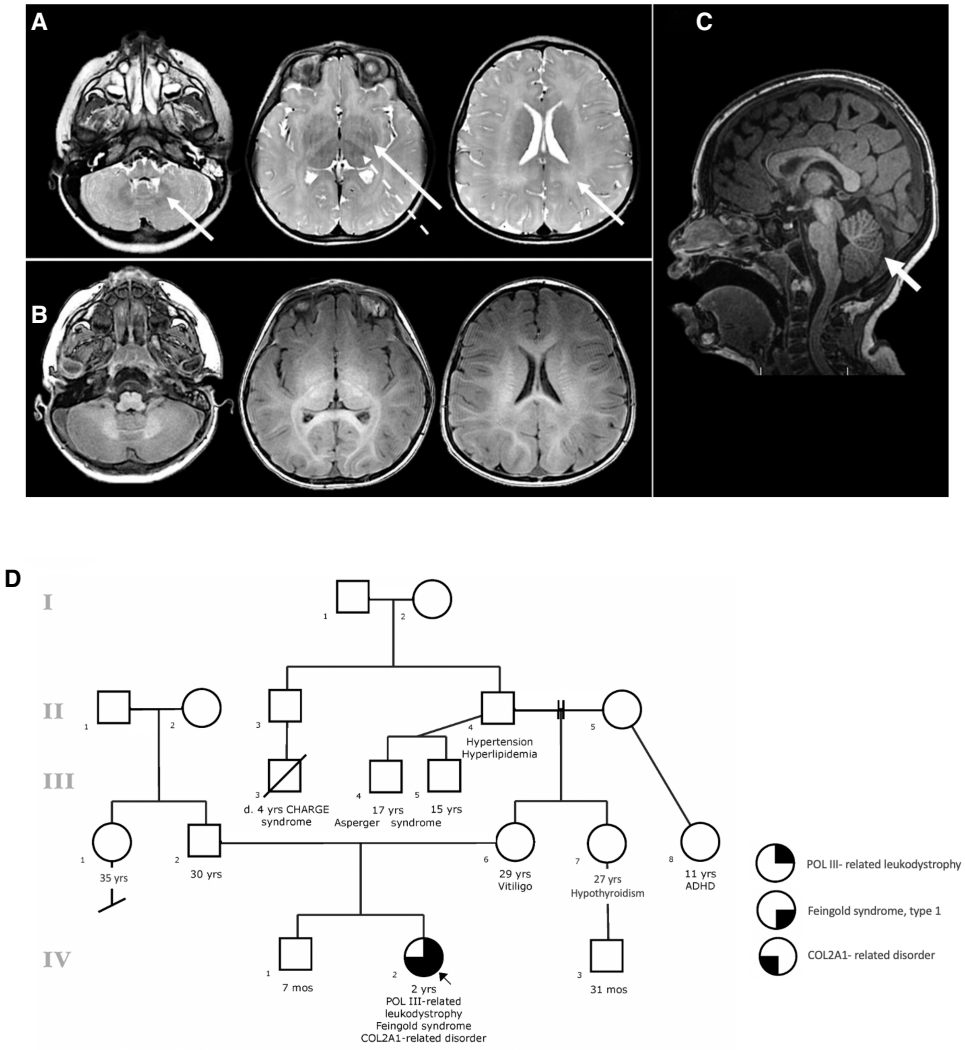

Figure 1. Proband brain imaging, family history, and a mosaic molecular finding. (*A–C*) Magnetic resonance imaging (MRI) obtained in 2-yr and 7-mo-old female. T2-weighted axial images (*A*) and T1-weighted images (*B*) demonstrate hypomyelination based on T2 hyperintensity and moderate T1 hyperintensity (arrow, *right* panel *A*), associated with relative T2-weighted hypointensity of the dentate (arrow, *left* panel *A*), the lateral thalamus (dotted arrow, *middle* panel *A*), and the medial globus pallidus (arrow, *middle* panel *A*). These findings are characteristic of Pol III–related disorders. Note that there is minimal to no cerebellar atrophy (short arrow, *C*). (*D*) Three-generation pedigree of the family (proband IV-2) obtained before diagnostic genome sequencing (GS) and modified after GS to include the proband's molecular diagnoses. No additional family updates were reported at the time of genetic result disclosure. (*E*) Representation of GS reads overlapping the *COL2A1* c.1693C > T variant for the proband, illustrating reduced number of reads containing the variant compared to the expected for a heterozygous germline variant. The region with the variant is highlighted in blue, the variant within each read is a green box, and red and blue reads illustrate strand direction. Please note, that the first green box appears transparent as it did not meet quality control metrics; thus, there are four quality reads.

Table 1. Molecular variant review

Gene/ transcript	Chromosomal variant coordinate (build 37.1)	HGVS DNA reference	HGVS protein reference	Variant type	Predicted effect	ACMG classification (criteria applied)	dbSNP/ dbVar ID	Genotype	ClinVar ID	Parent of origin	Previously described?	gnomAD all frequency (v2.1.1)	REVEL[a]
POLR3B NM_018082.6	Chr 12:106826199	c.1568T > A	p.Val523Glu	SNV	Missense	Pathogenic (PM3_very strong, PP2, PP4)	rs138249161	Heterozygous	SCV001251601.1	Paternal	Well known	0.0002903	0.76
POLR3B NM_018082.6	Chr 12:106848474	c.2278G > A	p.Ala760Thr	SNV	Missense	Likely pathogenic (PM2, PM3, PP2, PP4)	rs146513209	Heterozygous	SCV001251602.1	Maternal	Novel	0.00001419	0.77
COL2A1 NM_001844.5	Chr 12:48379358	c.1693C > T	p.Arg565Cys	SNV	Missense	Pathogenic (PS2, PS4, PM2)	rs121912884	Heterozygous	SCV001251606.1	De novo (mosaic)	Reported previously	Absent	0.69
Multiple, including *MYCN* NM_005378.5	seq[GRCh37]del(2)(2p24.3p24.1);Chr 2: g.15640273_19609496del	N/A	N/A	CNV	4-Mb loss	Pathogenic (N/A)	N/A	Heterozygous	SCV001754841	De novo	Novel	Absent	N/A

(HGVS) Human Genome Variation Society, (ACMG) American College of Medical Genetics and Genomics, (SNV) single-nucleotide variant, (N/A) not applicable, (CNV) copy-number variant.

[a]REVEL is an ensemble method for predicting the pathogenicity of missense variants on a basis of 13 individual tools: MutPred, FATHMM, VEST, PolyPhen, SIFT, PROVEAN, MutationAssessor, MutationTaster, LRT, GERP, SiPhy, phyloP, and phastCons. REVEL was trained on pathogenic and rare neutral missense variants, excluding those previously used to train its constituent tools. The REVEL score can range from 0 to 1, with higher scores predicting greater likelihood for the missense variant to be disease-causing.

Table 2. Variant detection capability by genetic testing modality

Variant	Chromosomal microarray	Leukodystrophy panel	ES	GS
4-Mb loss 2p24.3-p24.1 de novo	Detectable	Unlikely to be detected[a]	Potentially detectable[b]	Detectable
POLR3B CH pair of SNVs	Not detectable	Detectable	Detectable	Detectable
COL2A1 de novo SNV (mosaic)	Not detectable	Unlikely to be detected[a]	Potentially detectable[c]	Potentially detectable

(ES) Exome sequencing, (GS) genome sequencing, (CH) compound heterozygous, (SNV) single-nucleotide variant.
[a]The genes within the copy-number variant (CNV) have not been previously associated with a white matter disorder (Amberger et al. 2019; Martin et al. 2019), and *COL2A1* is not screened when white matter disorders are suspected.
[b]Because of uneven sequence coverage, frequent extension of CNVs beyond targeted regions, and lack of gold standard variants for validation, CNV detection in ES remains challenging (Pfundt et al. 2017; Bergant et al. 2018; Gordeeva et al. 2021). Clinical laboratories may not report CNVs via standard ES (Bergant et al. 2018; Burdick et al. 2020).
[c]Somatic variant detection by ES and GS depends on the location of the variant within the targeted region, coverage at the location, and laboratory metrics for reporting variants with low variant allele fraction (or alternate/reference allele ratio) (Wright et al. 2019).

trans with the known pathogenic variant p.Val523Glu, its presence in a gene with a low rate of benign missense variation and in which missense variants are a common mechanism, and the proband's phenotype including characteristic MRI findings with a clinically suspected leukodystrophy (Steenweg et al. 2010; Vrij-van den Bos et al. 2017).

The large 4-Mb de novo deletion of 2p24.3-p24.1 on Chromosome 2 (seq [GRCh37]del (2)(2p24.3p24.1); Chr 2:g.15640273_19609496del), affects 22 genes including a complete loss of the *MYCN* gene. *MYCN* haploinsufficiency is associated with Feingold syndrome, a disorder inherited in an autosomal dominant pattern that is typically characterized by microcephaly, hand, and foot abnormalities including fifth finger clinodactyly, small thumb, toe syndactyly, characteristic facial features including short palpebral fissures and micrognathia, learning disability, and gastrointestinal atresia (Marcelis and de Brouwer 2009). Additional features may include hearing loss, renal and cardiac malformations, and vertebral abnormalities. More than 100 affected individuals have been described to date, and penetrance appears to be 100%, but expressivity is variable. Intragenic and small deletions affecting *MYCN*, missense, nonsense, and frameshift variants have been described, with no recognizable difference in phenotypic features (Marcelis et al. 2008). With increasing size of the deletions and depending on their overall genetic content, additional variable phenotypes can be observed (Burnside et al. 2018). The CNV detected in this individual has not been previously reported in control or clinical populations, including DECIPHER, although larger and smaller deletions affecting the *MYCN* gene have been reported in individuals with features consistent with Feingold syndrome (Firth et al. 2009; Cooper et al. 2012; Macdonald et al. 2014; Landrum et al. 2016). This deletion was classified as pathogenic based on its de novo nature and identification of deletions including the *MYCN* gene in individuals with features of Feingold syndrome that overlap with the individual's phenotype, including microcephaly, intellectual disability, hearing impairment, micrognathia, brachymesophalangy of the second and the fifth fingers, and clinodactyly of the fifth finger (Fig. 2; Marcelis et al. 2008; Cognet et al. 2011; Chen et al. 2012).

The *COL2A1* gene encodes the α1 chain of collagen type II. Type II collagen, which is a large protein formed from homotrimers of α1 chains, is the main collagen secreted by chondrocytes that maintain the structure of connective tissues, such as hyaline cartilage, intervertebral discs, the vitreous humor of the eye, and the inner ear. Variants in the *COL2A1* gene cause *COL2A1*-related disorders including Stickler syndrome and type II collagenopathies,

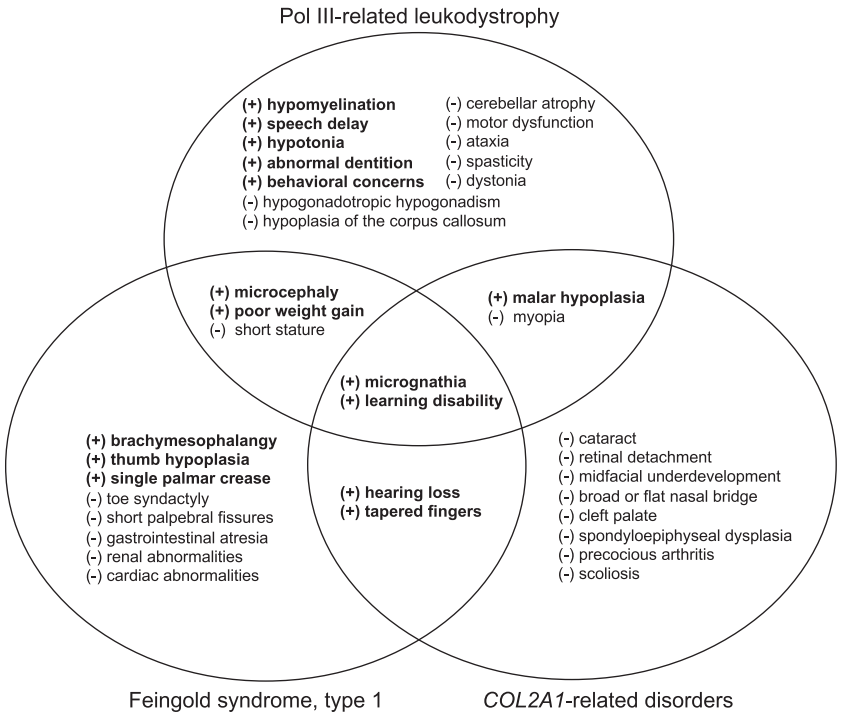

Figure 2. Venn diagram comparing the phenotypic spectrum of Feingold syndrome, *COL2A1*-related disorders, and Pol III–related leukodystrophy. The Venn diagram depicts the proband's clinical presentation observed up to the time of genetic result disclosure (+, bold). Clinical features associated with each condition but not observed in the proband (–, not bolded) are included to illustrate the medical complexity of each condition.

which are generally sporadic or inherited in an autosomal dominant manner. Stickler syndrome is a connective tissue disorder characterized by ocular involvement, conductive and sensorineural hearing loss, midface retrusion, cleft palate, mild spondyloepiphyseal dysplasia, and early-onset osteoarthritis (Robin et al. 2020–2021). It is primarily caused by loss of function variants in the *COL2A1* gene but may also result from missense variants. The type II collagenopathies include at least 16 clinically described disorders that are characterized by skeletal dysplasia, short stature, and sensory defects (Axél Gregersen and Savarirayan 1993). The clinical phenotypes associated with type II collagenopathies vary widely in severity and age of onset, with the most severe disorders resulting in death in utero or shortly after birth and the mildest not presenting until adulthood. Missense variants involving a substitution of a glycine residue in the triple helix domain, resulting in a dominant negative effect, are the most common cause of type II collagenopathies. A high degree of clinical variability is observed for *COL2A1*-related disorders, including across family members with the same variant (Robin et al. 2020–2021; Hoornaert et al. 2010; Kannu et al. 2011; Barat-Houari et al. 2016; Deng et al. 2016).

The *COL2A1* c.1693C > T (p.Arg565Cys) variant reported in this individual has a well-documented association with Stickler syndrome, having been reported in at least eight affected individuals, including one individual in whom the variant occurred de novo (Richards et al. 2000; Hoornaert et al. 2010; Wang et al. 2016; Zhou et al. 2018). In addition to vitreous anomalies, myopia, and other ophthalmological features, individuals with the p.Arg565Cys variant have been reported to show midface flattening, prominent eyes, low nasal bridge, and micrognathia. This variant is absent from gnomAD (v2.1.1, v3.1.1) and

results in the substitution of a cysteine for an arginine in the X position of the Gly–X–Y repeat of the triple helical domain. Variants in this position have been specifically linked to ocular phenotypes. The p.Arg565Cys variant was thus classified as pathogenic.

In the proband, a lower-than-expected number of reads supporting the variant suggested possible mosaicism. The total depth of sequencing coverage at this position was 24 reads. A germline heterozygous variant typically presents with close to 50% with a range of ~30%–70% of total depth corresponding to about seven to 17 reads. In this individual, we observed a total of four out of 24 (~17%) reads passing quality filters, suggesting mosaicism (Fig. 1E). This was assessed orthogonally using targeted variant testing with two alternative sets of primers, which confirmed the variant as mosaic. Mosaicism has been previously reported in at least eight individuals with *COL2A1*-related Stickler syndrome (Nagendran et al. 2012; Stevenson et al. 2012; Morrison et al. 2020; Yamamoto et al. 2020; Forzano et al. 2007; Winterpacht et al. 1993).

Implications for Clinical Management

Following molecular diagnosis, the individual was referred for evaluation by Ophthalmology and was advised to see Otorhinolaryngology. These evaluations were outstanding at the time of manuscript publication. Although there is no specific medication available to treat any of the three confirmed diagnoses, management guidance was shared with the family. Recommendations in the context of Pol III–related leukodystrophy included maintaining ambulation and weight bearing, regular maintenance labs for 25-OH-cholecalciferol and calcium, serial hip and spine X-rays, swallow studies, weight monitoring, baseline sleep study, baseline endocrine testing (TSH, T4, ACTH, cortisol, GH, and IGF1), and hormonal testing at the time of puberty (estrogens, progesterone, testosterone, LH, FSH). This individual will need to be followed yearly by endocrinology. Long-term management for this child will also need to include close follow-up with ophthalmology to detect ocular complications common to both *COL2A1*-related disorder and Pol III–related leukodystrophy. The individual continues to be followed by other specialist providers including neurology, otolaryngology, audiology, physical therapy, occupational therapy, and speech therapy.

DISCUSSION

In this report, three molecular diagnoses were identified in a single individual: Pol III–related leukodystrophy, Feingold syndrome, and *COL2A1*-related disorder. Although some of the individual's features can be uniquely ascribed to one of these conditions, overlap in the phenotypic contribution of each of the disorders makes it difficult to determine the relative impact of each variant to the overall clinical presentation (Fig. 2). For example, hypomyelination and white matter abnormalities, speech delay, hypotonia, and delayed primary dentition can be reasonably attributed to the *POLR3B* variants, whereas clinodactyly, rotated thumb, and simplified palmar crease are most likely the result of the 4-Mb deletion encompassing *MYCN*. Malar flattening, micrognathia, microcephaly, hearing loss, tapered fingers, and poor weight gain, however, overlap with more than one of the individual's molecular diagnoses. In addition, both the *POLR3B* and *COL2A1* variants may result in significant myopia.

At least five features observed in the individual were consistent with, but not unique to, *COL2A1*-related disorder. The *COL2A1* variant was identified in the individual's blood in ~17% (4/24) of total mapped reads passing quality filters. Because blood was the only tissue available for testing, whether the variant allele fraction was different in other tissues could not be evaluated because collection of other tissues would necessitate invasive procedures. Variability in the presence of mosaic variants across tissues has been associated with variable

expressivity (Gottlieb et al. 2001; Cao et al. 2019; Acierno et al. 2020; Martínez-Glez et al. 2020). Differences in expression of the mosaic *COL2A1* variant could provide an explanation for the absence of specific features of this disorder in the individual at the time of most recent evaluation.

There are few reports of individuals with mosaic, somatic *COL2A1* variants, making the contribution of *COL2A1* mosaic variants to the severity of associated clinical presentation difficult to discern. This report highlights the importance of mosaic variant identification and reporting, regardless of the clarity of the phenotypic contribution of the variant to the individual's overall presentation, as it can affect recurrence risk estimation and clinical surveillance recommendations. Current ACMG guidelines include only limited recommendations for the interpretation of mosaic variants (Richards et al. 2015). We argue that even if presentations are absent, mild, or inconsistent at the time of diagnosis, a mosaic variant classified as likely pathogenic or pathogenic should be returned to the family and followed up with genetic counseling, especially if there is a potential implication for family planning (Campbell et al. 2014; Rahbari et al. 2016; Breuss et al. 2020; Gambin et al. 2020). In this case, the family was able to be counseled on the negligent risk of recurrence to have another child with *COL2A1*-related disorder because the *COL2A1* variant was mosaic and de novo in the affected child. The child, however, would have a risk of recurrence that should be considered if/when they are older and planning a family. In addition, we recommend longitudinal follow-up visits to monitor for phenotype evolution in individuals with a mosaic variant, as proactive monitoring can be beneficial to an individual's overall medical management.

Whether mosaic variants of uncertain significance (VUSs) should be reported is much less clear. For some developmental conditions, a specific biomarker assay may help to classify an otherwise VUS mosaic variant. However, caution is needed when interpreting such assays because false-negative or intermediate results may lead to erroneous conclusions about variant pathogenicity (Choufani et al. 2015; Butcher et al. 2017; Wright et al. 2019). At the present time, in some cases clinical follow-up and detailed phenotyping may be the only option.

Although detection of mosaicism via GS is offered by some laboratories, it is not yet standard practice (Wright et al. 2019). This will likely become more frequent as variant calling improves and average read depth increases because of decreases in sequencing costs. As the number of individuals with mosaic variants reported through genome-wide sequencing increases, quantitative assessment of the link between variant allele fraction across tissues and its clinical impact will become possible (Campbell et al. 2014; Hochstenbach et al. 2014; Rahbari et al. 2016; Jónsson et al. 2018; Wright et al. 2019; Breuss et al. 2020; Gambin et al. 2020). We anticipate that some of the unexplained "missing diagnostic yield" and presumed genetic pleiotropy associated with some genetic conditions will be explained by previously undetected mosaic findings.

In summary, this report highlights the ability of GS to provide multiple molecular diagnoses, including those associated with a mosaic variant. Stepwise genetic testing in complex cases is the current standard of care and can be beneficial but may not capture all variants of interest. In a case such as the one presented in this report, sequential testing may have identified only a single diagnosis or provided a negative report that may have delayed or precluded additional genetic testing (Table 3; Helman et al. 2020).

Complex cases, such as the one presented here, prompt reconsideration of standard genetic testing procedures, test limitations, and outcomes in the context of individuals with complex clinical presentations and/or nonspecific findings. We argue that interpretation should not cease when variants that explain most of the phenotype are identified, as other variants, including both mosaic SNVs, CNVs, and repeat expansions, may contribute to the presentation.

Table 3. Individual genomic sequencing (GS) metrics

Metric		Value
Mean coverage		38.6×
Total reads		920,741,170
Total mapped reads		877,819,101
Read length		150 bp
SNV heterozygous/homozygous ratio		1.62
Read coverage	*COL2A1* c.1693C > T	24
	POLR3B c.1568T > A	32
	POLR3B c.2278G > A	31
Allele ratio (ALT/REF reads)	*COL2A1* c.1693C > T	0.1667 (4/20)
	POLR3B c.1568T > A	0.4688 (15/17)
	POLR3B c.2278G > A	0.5806 (18/13)
Variant QC metric (GQX[a])	*COL2A1* c.1693C > T	20
	POLR3B c.1568T > A	30
	POLR3B c.2278G > A	30

(SNV) Single-nucleotide variant, (QC) quality control.
[a]The GQX value is an empirically calibrated variant quality score for variant sites, intended to represent the minimum of {Phred genotype quality assuming the site is variant, Phred genotype quality assuming the site is nonvariant}.

METHODS

The individual was consented and enrolled in the Myelin Disorders Biorepository Project and LeukoSEQ at the Children's Hospital of Philadelphia. Clinical data was abstracted from available medical records, including postdiagnosis clinical management recommendation and neuroimaging.

Clinical trio GS was performed on DNA extracted from whole-blood samples collected from the proband and her parents. Extracted DNA was prepared for next-generation sequencing using the Illumina TruSeq PCR-free kit. Samples were sequenced on the Illumina HiSeq X system with paired-end 150-bp reads at the Illumina Clinical Services Laboratory in San Diego. Genome was sequenced to an average of ≥30-fold coverage (Table 2). The data were aligned (Raczy et al. 2013) according to build 37 of the Human Reference Genome (http://www.ncbi.nlm.nih.gov/projects/genome/assembly/grc/human) and analyzed using the Strelka caller for SNVs (Saunders et al. 2012) and Canvas caller for CNVs (Roller et al. 2016). Expansions of STRs were identified using ExpansionHunter (Dolzhenko et al. 2017).

Variants were filtered and prioritized based on multiple factors, including population allele frequency, variant consequence, evolutionary conservation, occurrence in a gene with a well-established gene–disease relationship, occurrence in a gene whose disease association overlaps the individual's reported phenotype, and inheritance, as appropriate. SNVs and CNVs were classified according to the ACMG guidelines current at the time of reporting (Kearney et al. 2011; Richards et al. 2015).

COL2A1 gene/targeted variant testing (GeneDx) was used to confirm the mosaic nature of the *COL2A1* c.1693C > T (p.Arg565Cys) variant. Using genomic DNA from the proband, the relevant portion of the *COL2A1* gene was polymerase chain reaction (PCR)-amplified, and capillary sequencing was performed. The bidirectional sequence was assembled, aligned to reference gene sequences based on human genome build GRCh37/UCSC hg19, and analyzed for the variant. The result was confirmed using alternative, nonoverlapping primers.

ADDITIONAL INFORMATION

Data Deposition and Access

All variants reported in this individual have been deposited in ClinVar (https://www.ncbi.nlm.nih.gov/clinvar/) under accession numbers SCV001251601.1 (*POLR3B* c.1568T > A), SCV001251602.1 (*POLR3B* c.2278G > A), SCV001251606.1 (*COL2A1* c.1693C > T), and SCV001754841 (seq[GRCh37]del(2)(2p24.3p24.1)).

Ethics Statement

The work presented in this report was performed under two research protocols approved by the Children's Hospital of Philadelphia IRB. Written informed consent and informed consent of parents for the child were obtained for enrollment in the Myelin Disorders Biorepository Project (IRB 14-011236) and for enrollment in GS through LeukoSEQ: Whole-Genome Sequencing as a First-Line Diagnostic Tool for Leukodystrophies (IRB 16-013213).

Acknowledgments

The authors offer thanks to this family for their participation in research and willingness to share their child's story for the benefit of the medical community. The authors also thank Vani Rajan for bioinformatic support.

Competing Interest Statement

R.J.T., A.R.C., Z.S., and D.L.P. are employees and shareholders of Illumina Inc. A.V. receives research support from Illumina, Takeda, Eli Lilly, Biogen, Passage Bio, and Homology.

Referees

Patrick J Morrison
Joshi Stephen
Anonymous

Received August 11, 2021; accepted in revised form November 2, 2021.

Author Contributions

K.J.M. and A.V. analyzed clinical data. A.R.C. analyzed and summarized genetic data for the GS report. Z.S. and R.T.H. reviewed genetic data and finalized the GS report. K.J.M., A.V., and Z.S. created the figures and tables. A.R.C., K.J.M., and Z.S. drafted the manuscript. A.V., H.D., D.L.P., R.T.H., and R.J.T. reviewed and revised the manuscript. All authors have approved the current version of the manuscript and its submission to *CSH Molecular Case Studies*.

Funding

A.V. and K.J.M. are supported by the Myelin Disorders Biorepository Project. The Myelin Disorders Biorepository Project is supported by the Children's Research Institute at the Children's Hospital of Philadelphia. Sequencing was provided by Illumina, Inc.

REFERENCES

Acierno JS, Xu C, Papadakis GE, Niederländer NJ, Rademaker JD, Meylan J, Messina A, Kolesinska Z, Quinton R, Lang-Muritano M, et al. 2020. Pathogenic mosaic variants in congenital hypogonadotropic hypogonadism. *Genet Med* **22:** 1759–1767. doi:10.1038/s41436-020-0896-0

Amberger JS, Bocchini C A, Scott AF, Hamosh A. 2019. OMIM.org: leveraging knowledge across phenotype–gene relationships. *Nucl Acids Res* **47:** D1038–D1043. doi:10.1093/nar/gky1151

Axél Gregersen P, Savarirayan R. 1993–2021. Type II Collagen Disorders Overview. *GeneReviews®*. https://www.ncbi.nlm.nih.gov/books/ (accessed August 4, 2021).

Balci TB, Hartley T, Xi Y, Dyment DA, Beaulieu C L, Bernier FP, Dupuis L, Horvath GA, Mendoza-Londono R, Prasad C, et al. 2017. Debunking Occam's razor: diagnosing multiple genetic diseases in families by whole-exome sequencing. *Clin Genet* **92:** 281–289. doi:10.1111/cge.12987

Barat-Houari M, Sarrabay G, Gatinois V, Fabre A, Dumont B, Genevieve D, Touitou I. 2016. Mutation update for *COL2A1* gene variants associated with type II collagenopathies. *Hum Mutat* **37:** 7–15. doi:10.1002/humu.22915

Battini R, Bertelloni S, Astrea G, Casarano M, Travaglini L, Baroncelli G, Pasquariello R, Bertini E, Cioni G. 2012. Longitudinal follow up of a boy affected by Pol III–related leukodystrophy: a detailed phenotype description. *BMC Med Genet* **16:** 1–8. doi:10.1186/s12881-015-0203-0

Bergant G, Maver A, Lovrecic L, Čuturilo G, Hodzic A, Peterlin B. 2018. Comprehensive use of extended exome analysis improves diagnostic yield in rare disease: a retrospective survey in 1,059 cases. *Genet Med* **20:** 303–312. doi:10.1038/gim.2017.142

Bernard G, Vanderver A. 2012–2017. POLR3-Related Leukodystrophy. *GeneReviews®*. https://www.ncbi.nlm.nih.gov/books/NBK99167/ (accessed July 19, 2021).

Breuss MW, Antaki D, George RD, Kleiber M, James KN, Ball LL, Hong O, Mitra I, Yang X, Wirth SA, et al. 2020. Autism risk in offspring can be assessed through quantification of male sperm mosaicism. *Nat Med* **26:** 143–150. doi:10.1038/s41591-019-0711-0

Burdick KJ, Cogan JD, Rives LC, Robertson AK, Koziura ME, Brokamp E, Duncan L, Hannig V, Pfotenhauer J, Vanzo R. 2020. Limitations of exome sequencing in detecting rare and undiagnosed diseases. *Am J Med Genet A* **182:** 1400–1406. doi:10.1002/ajmg.a.61558

Burnside RD, Molinari S, Botti C, Brooks SS, Chung WK, Mehta L, Schwartz S, Papenhausen P. 2018. Features of Feingold syndrome 1 dominate in subjects with 2p deletions including MYCN. *Am J Med Genet A* **176:** 1956–1963. doi:10.1002/ajmg.a.40355

Butcher DT, Cytrynbaum C, Turinsky AL, Siu MT, Inbar-Feigenberg M, Mendoza-Londono R, Chitayat D, Walker S, Machado J, Caluseriu O, et al. 2017. CHARGE and Kabuki syndromes: gene-specific DNA methylation signatures identify epigenetic mechanisms linking these clinically overlapping conditions. *Am J Hum Genet* **100:** 773–788. doi:10.1016/j.ajhg.2017.04.004

Campbell IM, Stewart JR, James RA, Lupski JR, Stankiewicz P, Olofsson P, Shaw CA. 2014. Parent of origin, mosaicism, and recurrence risk: probabilistic modeling explains the broken symmetry of transmission genetics. *Am J Hum Genet* **95:** 345–359. doi:10.1016/j.ajhg.2014.08.010

Cao Y, Tokita MJ, Chen ES, Ghosh R, Chen T, Feng Y, Gorman E, Gibellini F, Ward PA, Braxton A, et al. 2019. A clinical survey of mosaic single nucleotide variants in disease-causing genes detected by exome sequencing. *Genome Med* **11:** 48. doi:10.1186/s13073-019-0658-2

Chen C-P, Lin S-P, Chern S-R, Wu P-S, Chang S-D, Ng S-H, Liu Y-P, Su J-W, Wang W. 2012. A de novo 4.4-Mb microdeletion in 2p24.3→p24.2 in a girl with bilateral hearing impairment, microcephaly, digit abnormalities and Feingold syndrome. *Eur J Med Genet* **55:** 666–669. doi:10.1016/j.ejmg.2012.07.003

Choufani S, Cytrynbaum C, Chung B, Turinsky A, Grafodatskaya D, Chen Y, Cohen A, Dupuis L, Butcher D, Siu M, et al. 2015. *NSD1* mutations generate a genome-wide DNA methylation signature. *Nat Commun* **6:** 10207. doi:10.1038/ncomms10207

Cognet M, Nougayrede A, Malan V, Callier P, Cretolle C, Faivre L, Genevieve D, Goldenberg A, Heron D, Mercier S, et al. 2011. Dissection of the *MYCN* locus in Feingold syndrome and isolated oesophageal atresia. *Eur J Hum Genet* **19:** 602–606. doi:10.1038/ejhg.2010.225

Cooper GM, Coe BP, Girirajan S, Rosenfeld JA, Vu T, Baker C, Williams C, Stalker H, Hamid R, Hannig V, et al. 2012. A copy number variation morbidity map of developmental delay. *Nat Genet* **43:** 838–846. doi:10.1038/ng.909

Daoud H, Tétreault M, Gibson W, Guerrero K, Cohen A, Gburek-Augustat J, Synofzik M, Brais B, Stevens CA, Sanchez-Carpintero R, et al. 2013. Mutations in *POLR3A* and *POLR3B* are a major cause of hypomyelinating leukodystrophies with or without dental abnormalities and/or hypogonadotropic hypogonadism. *J Med Genet* **50:** 194–197. doi:10.1136/jmedgenet-2012-101357

Deng H, Huang X, Yuan L. 2016. Molecular genetics of the *COL2A1*-related disorders. *Mutat Res* **768:** 1–13. doi:10.1016/j.mrrev.2016.02.003

Dolzhenko E, van Vugt JJFA, Shaw RJ, Bekritsky MA, van Blitterswijk M, Narzisi G, Ajay SS, Rajan V, Lajoie BR, Johnson NH, et al. 2017. Detection of long repeat expansions from PCR-free whole-genome sequence data. *Genome Res* **27:** 1895–1903. doi:10.1101/gr.225672.117

Ferrer A, Schultz-Rogers L, Kaiwar C, Kemppainen JL, Klee EW, Gavrilova RH. 2019. Three rare disease diagnoses in one patient through exome sequencing. *Cold Spring Harb Mol Case Stud* **5:** a004390. doi:10.1101/mcs.a004390

Firth HV, Richards SM, Bevan AP, Clayton S, Corpas M, Rajan D, van Vooren S, Moreau Y, Pettett RM, Carter NP. 2009. DECIPHER: Database of Chromosomal Imbalance and Phenotype in Humans using Ensembl Resources. *Am J Hum Genet* **84:** 524–533. doi:10.1016/j.ajhg.2009.03.010

Forzano F, Lituania M, Viassolo V, Superti-Furga A, Wildhardt G, Zabel B, Faravelli F. 2007. A familial case of achondrogenesis type II caused by a dominant *COL2A1* mutation and ''patchy'' expression in the mosaic father. *Am J Med Genet A* **143:** 2815–2820.

Gambin T, Liu Q, Karolak JA, Grochowski CM, Xie NG, Wu LR, Yan YH, Cao Y, Coban Akdemir ZH, Wilson TA, et al. 2020. Low-level parental somatic mosaic SNVs in exomes from a large cohort of trios with diverse suspected Mendelian conditions. *Genet Med* **22:** 1768–1776. doi:10.1038/s41436-020-0897-z

Gordeeva V, Sharova E, Babalyan K, Sultanov R, Govorun VM, Arapidi G. 2021. Benchmarking germline CNV calling tools from exome sequencing data. *Sci Rep* **11:** 14416. doi:10.1038/s41598-021-93878-2

Gottlieb B, Beitel LK, Trifiro MA. 2001. Somatic mosaicism and variable expressivity. *Trends Genet* **17:** 79–82. doi:10.1016/S0168-9525(00)02178-8

Gross AM, Ajay SS, Rajan V, Brown C, Bluske K, Burns NJ, Chawla A, Coffey AJ, Malhotra A, Scocchia A, et al. 2019. Copy-number variants in clinical genome sequencing: deployment and interpretation for rare and undiagnosed disease. *Genet Med* **21:** 1121–1130. doi:10.1038/s41436-018-0295-y

Helman G, Lajoie BR, Crawford J, Takanohashi A, Walkiewicz M, Dolzhenko E, Gross AM, Gainullin VG, Bent SJ, Jenkinson EM, et al. 2020. Genome sequencing in persistently unsolved white matter disorders. *Ann Clin Transl Neurol* **7:** 144–152. doi:10.1002/acn3.50957

Hochstenbach R, Krijtenburg P-J, van der Veken LT, van der Smagt J, Roeleveld-Versteegh A, Visser G, Terhal P. 2014. Monosomy 20 mosaicism revealed by extensive karyotyping in blood and skin cells: case report and review of the literature. *Cytogenet Genome Res* **144:** 155–162. doi:10.1159/000369606

Hoornaert KP, Vereecke I, Dewinter C, Rosenberg T, Beemer FA, Leroy JG, Bendix L, Björck E, Bonduelle M, Boute O, et al. 2010. Stickler syndrome caused by *COL2A1* mutations: genotype and phenotype correlation in a series of 100 patients. *Eur J Hum Genet* **7:** 872–881. doi:10.1038/ejhg.2010.23

Jehee FS, de Oliveira VT, Gurgel-Giannetti J, Pietra RX, Rubatino FV, Carobin NV, Vianna GS, de Freitas ML, Fernandes KS, Ribeiro BS, et al. 2017. Dual molecular diagnosis contributes to atypical Prader–Willi phenotype in monozygotic twins. *Am J Med Genet A* **173:** 2451–2455. doi:10.1002/ajmg.a.38315

Jónsson H, Sulem P, Arnadottir GA, Pálsson G, Eggertsson HP, Kristmundsdottir S, Zink F, Kehr B, Hjorleifsson KE, Jensson B Ö, et al. 2018. Multiple transmissions of de novo mutations in families. *Nat Genet* **50:** 1674–1680. doi:10.1038/s41588-018-0259-9

Kannu P, Bateman J, Savarirayan R. 2011. Clinical phenotypes associated with type II collagen mutations. *J Paediatr Child Health* **48:** E38–E43. doi:10.1111/j.1440-1754.2010.01979.x

Kearney HM, Thorland EC, Brown KK, Quintero-Rivera F, South ST. 2011. American College of Medical Genetics standards and guidelines for interpretation and reporting of postnatal constitutional copy number variants. *Genet Med* **13:** 680–685. doi:10.1097/GIM.0b013e3182217a3a

Kuczmarski RJ, Ogden CL, Guo SS, Grummer-Strawn LM, Flegal KM, Mei Z, Wei R, Curtin LR, Roche AF, Johnson CL. 2002. 2000 CDC Growth Charts for the United States: methods and development. *Vital Health Stat* **11:** 1–190.

Landrum MJ, Lee JM, Benson M, Brown G, Chao C, Chitipiralla S, Gu B, Hart J, Hoffman D, Hoover J, et al. 2016. ClinVar: public archive of interpretations of clinically relevant variants. *Nucl Acids Res* **44:** D862–D868. doi:10.1093/nar/gkv1222

MacDonald JR, Ziman R, Yuen RKC, Feuk L, Scherer SW. 2014. The Database of Genomic Variants: a curated collection of structural variation in the human genome. *Nucl Acids Res* **42:** D986–D992. doi:10.1093/nar/gkt958

Manickam K, Mcclain MR, Demmer LA, Biswas S, Kearney HM, Malinowski J, Massingham LJ, Miller D, Yu TW, Hisama FM, et al. 2021. Exome and genome sequencing for pediatric patients with congenital anomalies or intellectual disability: an evidence-based clinical guideline of the American College of Medical Genetics and Genomics (ACMG). *Genet Med* **23:** 2029–2037. doi: 10.1038/s41436-021-01242-6

Marcelis C, de Brouwer A. 2009–2019. Feingold Syndrome 1. *GeneReviews®*. https://www.ncbi.nlm.nih.gov/books/NBK7050/ (Accessed July 19, 2021).

Marcelis CLM, Hol FA, Graham GE, Rieu PNMA, Kellermayer R, Meijer RPP, Lugtenberg D, Scheffer H, van Bokhoven H, Brunner HG, et al. 2008. Genotype–phenotype correlations in *MYCN*-related Feingold syndrome. *Hum Mutat* **29:** 1125–1132. doi:10.1002/humu.20750

Martin AR, Williams E, Foulger RE, Leigh S, Daugherty LC, Niblock O, Leong IUS, Smith KR, Gerasimenko O, Haraldsdottir E, et al. 2019. PanelApp crowdsources expert knowledge to establish consensus diagnostic gene panels. *Nat Genet* **51:** 1560–1565. doi:10.1038/s41588-019-0528-2

Martínez-Glez V, Tenorio J, Nevado J, Gordo G, Rodríguez-Laguna L, Feito M, de Lucas R, Pérez-Jurado LA, Ruiz Pérez VL, Torrelo A, et al. 2020. A six-attribute classification of genetic mosaicism. *Genet Med* **22:** 1743–1757. doi:10.1038/s41436-020-0877-3

Miller CR, Lee K, Pfau RB, Reshmi SC, Corsmeier DJ, Hashimoto S, Dave-Wala A, Jayaraman V, Koboldt D, Matthews T, et al. 2020. Disease-associated mosaic variation in clinical exome sequencing: a two-year pediatric tertiary care experience. *Cold Spring Harb Mol Case Stud* **6:** a005231. doi:10.1101/mcs.a005231

Morrison PJ, Znaczko A, Jansson M. 2020. Paternal somatogonadal *COL2A1* mosaicism causing recurrence of severe type 2 collagenopathy. *Am J Med Genet A* **182:** 2191–2194.

Nagendran S, Richards AJ, Mcninch A, Sandford RN, Snead MP. 2012. Somatic mosaicism and the phenotypic expression of *COL2A1* mutations. *Am J Med Genet A* **158:** 1204–1207.

Posey JE, O'Donnell-Luria AH, Chong JX, Harel T, Jhangiani SN, Coban Akdemir ZH, Buyske S, Pehlivan D, Carvalho CM B, Baxter S, et al. 2019. Insights into genetics, human biology and disease gleaned from family based genomic studies. *Genet Med* **21:** 798–812. doi:10.1038/s41436-018-0408-7

Posey JE, Rosenfeld JA, James RA, Bainbridge M, Niu Z, Wang X, Dhar S, Wiszniewski W, Akdemir ZHC, Gambin T, et al. 2016. Molecular diagnostic experience of whole-exome sequencing in adult patients. *Genet Med* **18:** 678–685. doi:10.1038/gim.2015.142

Pfundt R, del Rosario M, Vissers L ELM, Kwint MP, Janssen IM, de Leeuw N, Yntema HG, Nelen MR, Lugtenberg D, Kamsteeg E-J, et al. 2017. Detection of clinically relevant copy-number variants by exome sequencing in a large cohort of genetic disorders. *Genet Med* **19:** 667–675. doi:10.1038/gim.2016.163

Raczy C, Petrovski R, Saunders CT, Chorny I, Kruglyak S, Margulies EH, Chuang H-Y, Källberg M, Kumar SA, Liao A, et al. 2013. Isaac: ultra-fast whole-genome secondary analysis on Illumina sequencing platforms. *Bioinformatics* **29:** 2041–2043. doi:10.1093/bioinformatics/btt314

Rahbari R, Wuster A, Lindsay SJ, Hardwick RJ, Alexandrov LB, Al Turki S, Dominiczak A, Morris A, Porteous D, Smith B, et al. 2016. Timing, rates and spectra of human germline mutation. *Nat Genet* **48:** 126–133. doi:10.1038/ng.3469

Richards AJ, Baguley DM, Yates JRW, Lane C, Nicol M, Harper PS, Scott JD, Snead MP. 2000. Variation in the vitreous phenotype of stickler syndrome can be caused by different amino acid substitutions in the X position of the type II collagen Gly–X–Y triple helix. *Am J Hum Genet* **67:** 1083–1094. doi:10.1086/321189

Richards S, Aziz N, Bale S, Bick D, Das S, Gastier-Foster J, Grody WW, Hegde M, Lyon E, Spector E, et al. 2015. *Standards and guidelines for the interpretation of sequence variants: a joint consensus recommendation of the* American College of Medical Genetics and Genomics and the Association for Molecular Pathology. *Genet Med* **17:** 405–424. doi:10.1038/gim.2015.30

Robin NH, Moran RT, Ala-Kokko L. 2000–2021. Stickler Syndrome. *GeneReviews®*. https://www.ncbi.nlm.nih.gov/books/NBK1302/ (accessed August 3, 2021).

Rodin RE, Dou Y, Kwon M, Sherman MA DAM, Doan RN, Rento LM, Girskis KM, Bohrson CL, Kim SN, et al. 2021. The landscape of somatic mutation in cerebral cortex of autistic and neurotypical individuals revealed by ultra-deep whole-genome sequencing. *Nat Neurosci* **24:** 176–185. doi:10.1038/s41593-020-00765-6

Roller E, Ivakhno S, Lee S, Royce T, Tanner S. 2016. Canvas: versatile and scalable detection of copy number variants. *Bioinformatics* **32:** 2375–2377. doi:10.1093/bioinformatics/btw163

Saunders CT, Wong WSW, Swamy S, Becq J, Murray LJ, Cheetham RK. 2012. Strelka: accurate somatic small-variant calling from sequenced tumor–normal sample pairs. *Bioinformatics* **28:** 1811–1817. doi:10.1093/bioinformatics/bts271

Smith ED, Blanco K, Sajan SA, Hunter JM, Shinde DN, Wayburn B, Rossi M, Huang J, Stevens CA, Muss C, et al. 2019. A retrospective review of multiple findings in diagnostic exome sequencing: half are distinct and half are overlapping diagnoses. *Genet Med* **21:** 2199–2207. doi:10.1038/s41436-019-0477-2

Steenweg ME, Vanderver A, Blaser S, Bizzi A, de Koning TJ, Mancini GMS, van Wieringen WN, Barkhof F, Wolf NI, van der Knaap MS. 2010. Magnetic resonance imaging pattern recognition in hypomyelinating disorders. *J Neurol* **133:** 2971–2982. doi:10.1093/brain/awq257

Stevenson DA, Vanzo R, Damjanovich K, Hanson H, Muntz H, Hoffman RO, Bayrak-Toydemir P. 2012. Mosaicism in Stickler syndrome. *Eur J Med Genet* **55:** 418–422.

Vanderver A, Bernard G, Helman G, Sherbini O, Boeck R, Cohn J, Collins A, Demarest S, Dobbins K, Emrick L, et al. 2020. Randomized clinical trial of first-line genome sequencing in pediatric white matter disorders. *Ann Neurol* **88:** 264–273. doi:10.1002/ana.25757

Vrij-van den Bos S, Hol JA, La Piana R, Harting I, Vanderver A, Barkhof F, Cayami F, van Wieringen WN, Pouwels PJW, van der Knaap MS, et al. 2017. 4H leukodystrophy: a brain magnetic resonance imaging scoring system. *Neuropediatrics* **48:** 152–160. doi:10.1055/s-0037-1599141

Wang X, Jia X, Xiao X, Li S, Li J, Li Y, Wei Y, Liang X, Guo X. 2016. Mutation survey and genotype–phenotype analysis of *COL2A1* and *COL11A1* genes in 16 Chinese patients with Stickler syndrome. *Mol Vis* **22:** 697–704.

Winterpacht A, Hilbert M, Schwarze U, Mundlos S, Spranger J, Zabel BU. 1993. Kniest and Stickler dysplasia phenotypes caused by collagen type II gene (*COL2A1*) defect. *Nat Genet* **3:** 323–326.

Wolf NI, Vanderver A, van Spaendonk RM, Schiffmann R, Brais B, Bugiani M, Sistermans E, Catsman-Berrevoets C, Kros JM, Soares Pinto P, et al. 2014. Clinical spectrum of 4H leukodystrophy caused by POLR3A and *POLR3B* mutations. *Neurology* **83:** 1898–1905. doi:10.1212/WNL.0000000000001002

Wright CF, Prigmore E, Rajan D, Handsaker J, Mcrae J, Kaplanis J, Fitzgerald TW, Fitzpatrick DR, Firth H, Hurles ME. 2019. Clinically-relevant postzygotic mosaicism in parents and children with developmental disorders in trio exome sequencing data. *Nat Commun* **10:** 2985. doi:10.1038/s41467-019-11059-2

Yamamoto K, Kubota T, Takeyari S, Kitaoka T, Miyata K, Nakano Y, Nakayama H, Ohata Y, Yanagi K, Kaname T, et al. 2020. Parental somatogonadal *COL2A1* mosaicism contributes to intrafamilial recurrence in a family with type 2 collagenopathy. *Am J Med Genet A* **182:** 454–460.

Yang Y, Muzny D, Reid J, Bainbridge M, Willis A, Ward P, Braxton A, Beuten J, Xia F, Niu ZN, et al. 2013. Clinical whole-exome sequencing for the diagnosis of Mendelian disorders. *N Engl J Med* **369:** 1502–1511. doi:10.1056/NEJMoa1306555

Yang Y, Muzny DM, Xia F, Niu Z, Person R, Ding Y, Ward P, Braxton A, Wang M, Buhay C, et al. 2014. Molecular findings among patients referred for clinical whole-exome sequencing. *J Am Med Assoc* **312:** 1870–1879. doi:10.1001/jama.2014.14601

Zhou L, Xiao X, Li S, Jia X, Wang P, Sun W, Zhang F, Li J, Li T, Zhang Q. 2018. Phenotypic characterization of patients with early-onset high myopia due to mutations in *COL2A1* or *COL11A1*: why not Stickler syndrome? *Mol Vis* **24:** 560–573.